Singlet–triplet energy separations in divalent five-membered cyclic conjugated C_5H_3X, C_4H_3SiX, C_4H_3GeX, C_4H_3SnX, and C_4H_3PbX (X = H, F, Cl, and Br)

M.Z. Kassaee *, S. Arshadi, M. Acedy, E. Vessally

Department of Chemistry, University of Tarbiat Modarres, Pole-Ghisha, Chamran High Way, P.O. Box 14155-4838, Tehran, Iran

Abstract

Singlet–triplet energy gaps in cyclopenta-2,4-dienylidene, as well as its 2- or 3-halogenated derivatives, are compared and contrasted with their sila, germa, stana, and plumba analogues; at HF/6-31G* and B3LYP/ 6-311++G(3df, 2p) levels of theory. Energy gaps (ΔG_{t-s}), between triplet (t) and singlet (s) states, appear linearly proportional to: (i) the size of the group 14 divalent element (M = C, Si, Ge, Sn and Pb), (ii) the angle $\angle$C–M–C, and (iii) the $\Delta G_{(LUMO-HOMO)}$ of the singlet state involved. The magnitude of ΔG_{t-s}, for each 2- and/or 3-substituted species studied, increases with an order of: carbenes < silylenes < germylenes < stanylenes < plumbylenes. This order reverses for the barriers of the ring puckering. The puckering occurs with more ease for every singlet, compared to its corresponding triplet form.

Regardless of the group 14 element (M) employed, every 3-halo-substituted species is more stable than the corresponding 2-halo-substituted isomer. For M = Pb, Sn and/or Ge; 3-halo-substituted species have higher ΔG_{t-s} than their corresponding 2-halo-substituted analogues. For M = Si, similar ΔG_{t-s} are found for 2- and 3-halogenated isomers. For M = C, 3-halo-substituted species have lower ΔG_{t-s} than their corresponding 2-halo-substituted analogues.

Every cyclic singlet has a larger $\angle$C–M–C angle, than its corresponding cyclic triplet state, except for 3-halosilacyclopenta-2,4-dienylidenes where triplet has a larger $\angle$C–M–C angle than its corresponding singlet state.
© 2005 Elsevier B.V. All rights reserved.

Keywords: Carbenes; Silylenes; Germylenes; Stanylenes; Plumbylenes; Singlet–triplet energy gap; C_5H_4; C_4H_4Si; C_4H_4Ge; C_4H_4Sn; C_4H_4Pb

1. Introduction

Divalent carbenes and their heavier analogues are intensely reactive, and the studies of their properties are often made through matrix isolation techniques [1]. Among the relatively more stable carbenes, the cyclic completely conjugated species, and their halogenated derivatives, have held a special place in the chemistry of divalent carbon intermediates (Scheme 1) [2]. These divalent structures were formerly described in terms of the Huckel $4n + 2$ rule [3]. However, semi-empirical studies found most of these singlets, planar, cyclic conjugated carbenes not to be energy minima, suggesting non-planar isomers to be considered [4]. Arduengo and co-workers [5] reported the isolation of the stable cyclic conjugated carbene, 1,3-di(1-adamantyl)imidazol-2-ylidene. Subsequently, the stable cyclic singlet silylenes, 1 and 2 [6], and the corresponding germylenes, 3 and 4 [7] were synthesized and their physical properties were compared to the Arduengo-type carbenes 5 and 6 [8] (Scheme 2). Robert West and co-workers [8a] studied stable 1, 2, 3, and 4, computationally and by cyclic voltammetry (CV). They attributed the unusual stability of the unsaturated silylene 1 toward reduction to its

---

* Corresponding author. Fax: +98 21 8006544.
 E-mail addresses: kassaeem@modares.ac.ir, Drkassaee@yahoo.com (M.Z. Kassaee).
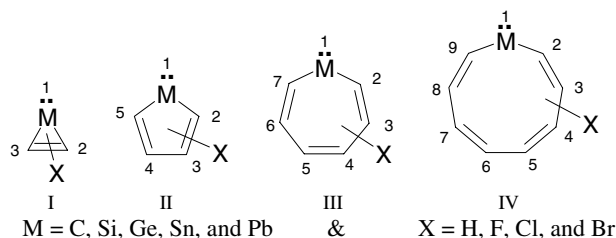
Scheme 1. Group 14 divalent (M) species confined into X-substituted completely conjugated 3-, 5-, 7-, and 9-membered rings, for M = C, Si, Ge, Sn, Pb; and X = H, F, Cl, Br [3,6a,8c].
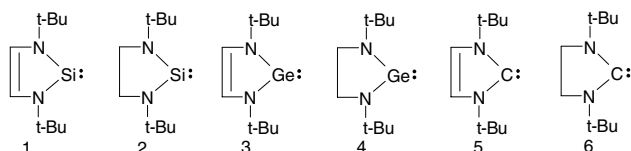
Scheme 2. Stable cyclic silylenes (1 and 2 [6]), and germylenes (3 and 4 [7]), are comparable to the stable carbenes 5 and 6 [8].

aromatic (6π electrons) stabilization. Evidently, some of these halo-species play a role as important intermediates in organic synthesis and in gas-phase combustion [9]. Moreover, halo-carbenes are one set of possible photo-products from the breakdown of both hydro-chlorofluorocarbons (HCFCs) and halons in atmosphere.

Silylenes and to a lesser extent germylenes, have been the center of attention over the last two decades, due to the importance of these group 14 electron-deficient radicals in chemical vapor deposition, semiconductor manufacture, and the photonics and aerospace industries [10,11]. In particular, the oxidation chemistry of silylene has received considerable attention, both experimentally and theoretically [12]. Particularly, silylene is well-known to insert into O–H bonds [13].

In addition, considerable progress has been made in the chemistry of stable organic derivatives of divalent tin [14]. Radicals, ions, ion radicals of stanylenes have been suggested as intermediates in redox reactions of diazo compounds and other molecules, both in the liquid and gas phases [15].

Finally, the heaviest carbene analogues "plumbylenes", appear less well-known. Isolation of the plumbyl-

enes and the characterization of their derivatives are reported [16,17]. They usually occur as reactive intermediates in the preparation of plumbanes, R_4Pb, and polymerize and undergo disproportionation in the absence of suitable stabilizing groups on the lead atom [18]. The *t*-Bu group may be employed as a stabilizer for a variety of highly reactive plumbylenes [19].

Following up on our quest for more stable halogenated group 14 divalent species [2,4], in this manuscript we have carried out ab initio and DFT comparative studies on four possible configurations (σ^2 ($^1A_1$), singlet; P^2 ($^1B_1$), singlet; σ^1P^1 ($^1B_1$), singlet; and σ^1P^1 ($^3B_1$), triplet) [20] for completely conjugated X-cyclopenta-2,4-dienylidenes (M = C; X = H, F, Cl, and Br) as well as their group 14 divalent homologues (M = Si, Ge, Sn, and Pb) (Scheme 3).

2. Computational methods

Geometry optimizations are carried out by HF and DFT (B3LYB) methods [21,22]. This is using 6-31G* basis set of the GAUSSIAN 98 system of programs [23].
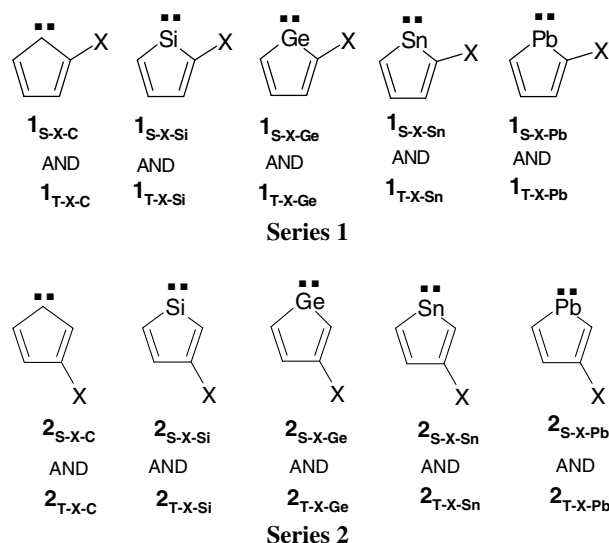
Fig. 1. Homologues divalent species of group 14 in the periodic table: two series (Series 1 and 2) of halogenated cyclic carbenes, silylenes, germylenes, stanylenes and plumbylenes.
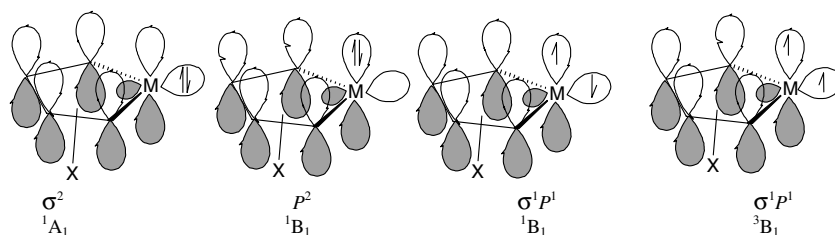
Scheme 3. Possible configurations for 2X- and/or 3X-cyclopenta-2,4-dienylidenes and their group 14 divalent homologues are: σ^2 ($^1A_1$), singlet; P^2 ($^1B_1$), singlet; σ^1P^1 ($^1B_1$), singlet; and σ^1P^1 ($^3B_1$), triplet, for M = C, Si, Ge, Sn, and Pb (X = H, F, Cl, Br).

Global minima are specified on corresponding energy surfaces through relax scan using Keyword "FOPT (Z-matrix)" at B3LYP/6-311++G (3df, 2p) level of theory. Obtained minimum via scanning, the latter are used as inputs for the B3LYB/6-311++G (3df, 2p) (basis set of McGrath, Curtiss included the diffuse functions) calculations. This is for obtaining more accurate values of change of electronic and thermal energies ($\Delta E_{(t-s)}$), enthalpies ($\Delta H_{(t-s)}$) and Gibbs free energies ($\Delta G_{(t-s)}$). For stanylenes and plumbylenes that have hetro-atoms, such Sn and Pb, calculation using McGrath, Curtiss basis set are done via "Extrabasis" keyword (hetro-atoms are optimized using LANEL2DZ basis set) [24]. To confirm the nature of the stationary species, frequency calculations are carried out. For minimum state structures, only real frequency values are accepted. Thermodynamic functions obtained through frequency calculations, are multiplied by the scaling factor and correction terms. In order to obtain the three dimensional iso-surface HOMO plots for triplet silylene, triplet germylene, singlet silylenes, and singlet germylene, UB3LYP/6-311++G** calculated data in GAUSSIAN 98 system of programs are inputted as a script for Hyperchem software. The nature of HOMO for all species, are plotted using Hyperchem software as shown in three dimensional isosurface formats.

In order to perform solvation analysis of structures in Series 1 and 2, their optimizations are carried out in chloroform, using the "Polarizable Continuum Solvation Model" (PCSM) [25,26].

3. Results and discussion

An attempt is made to enlist all the results, before opening the discussion. Hence, singlet–triplet energy

Table 1

Calculated B3LYP/6-311++G(3df, 2p) sum of electronic and thermal energies (E), sum of electronic and thermal enthalpies (H), sum of electronic and thermal Gibbs free energies (G) and zero-point energies (ZPE) for singlet and triplet states of sila-, germa-, stana-, and plumba-2-X-cyclopenta-2,4-dienylidenes [(1_{S-X-C} vs. 1_{T-X-C}), (1_{S-X-Si} vs. 1_{T-X-Si}), (1_{S-X-Ge} vs. 1_{T-X-Ge}) (1_{S-X-Sn} vs. 1_{T-X-Sn}), and (1_{S-X-Pb} vs. 1_{T-X-Pb}), respectively: Series 1], where X = H, F, Cl and Br

Compound(s)	E	H	G	ZPE
1_{S-H-C}	−192.741508	−192.740563	−192.771540	41.16
1_{S-F-C}	−292.009057	−292.008113	−292.041710	37.22
1_{S-Cl-C}	−652.368109	−652.367165	−652.402159	36.23
1_{S-Br-C}	−2766.289104	−2766.288160	−2766.324547	35.84
1_{T-H-C}	−192.755824	−192.754880	−192.787203	41.86
1_{T-F-C}	−292.025609	−292.024665	−292.059356	36.84
1_{T-Cl-C}	−652.384179	−652.383234	−652.419252	35.98
1_{T-Br-C}	−2766.304890	−2766.303946	−2766.341348	35.61
1_{S-H-Si}	−444.213931	−444.212987	−444.247502	39.88
1_{S-F-Si}	−543.487414	−543.48647	−543.523306	34.95
$1_{S-Cl-Si}$	−903.848484	−903.84754	−903.885721	34.16
$1_{S-Br-Si}$	−3017.770015	−3017.769071	−3017.808686	33.80
1_{T-H-Si}	−444.178936	−444.177992	−444.213174	39.17
1_{T-F-Si}	−543.457556	−543.456612	−543.492810	35.24
$1_{T-Cl-Si}$	−903.825423	−903.824479	−903.861842	34.43
$1_{T-Br-Si}$	−3017.741529	−3017.740585	−3017.779429	34.12
1_{S-H-Ge}	−2231.734466	−2231.733521	−2231.769057	39.43
1_{S-F-Ge}	−2331.006873	−2331.005929	−2331.043823	34.51
$1_{S-Cl-Ge}$	−2691.372492	−2691.371547	−2691.410559	33.74
$1_{S-Br-Ge}$	−4805.289527	−4805.288583	−4805.329135	33.39
1_{T-H-Ge}	−2231.696392	−2231.695468	−2231.731744	38.60
1_{T-F-Ge}	−2330.976543	−2330.975599	−2331.013969	34.10
$1_{T-Cl-Ge}$	−2691.331320	−2691.330375	−2691.370196	32.84
$1_{T-Br-Ge}$	−4805.257368	−4805.256424	−4805.297508	32.94
1_{S-H-Sn}	−158.107281	−158.106336	−158.142542	39.13
1_{S-F-Sn}	−170.626652	−170.6295708	−170.67078	33.09
$1_{S-Cl-Sn}$	−172.482038	−172.481094	−172.520897	32.78
$1_{S-Br-Sn}$	−257.382169	−257.381225	−257.419988	34.19
1_{T-H-Sn}	−158.062985	−158.062041	−158.099348	38.08
1_{T-F-Sn}	−170.657981	−170.657036	−170.699248	32.5
$1_{T-Cl-Sn}$	−172.414998	−172.414054	−172.454886	32.12
$1_{T-Br-Sn}$	−257.345419	−257.344475	−257.383944	33.62
1_{S-H-Pb}	−158.20208	−158.201136	−158.238261	38.86
1_{S-F-Pb}	−170.792862	−170.791918	−170.834252	32.86
$1_{S-Cl-Pb}$	−172.574822	−172.573878	−172.614855	33.2
$1_{S-Br-Pb}$	−257.47818	−257.477236	−257.51693	33.96
1_{T-H-Pb}	−158.147507	−158.146563	−158.184305	37.83
1_{T-F-Pb}	−170.751848	−170.750904	−170.79413	32.19
$1_{T-Cl-Pb}$	−172.534129	−172.533185	−172.57502	32.55
$1_{T-Br-Pb}$	−257.439244	−257.4383	−257.478777	33.33

Table 2

Calculated B3LYP/6-311++G(3df, 2p) sum of electronic and thermal energies (E), sum of electronic and thermal enthalpies (H), sum of electronic and thermal Gibbs free energies (G) and zero-point energies (ZPE) for singlet and triplet states of sila-, germa-, stana-,and plumba-3-X-cyclopenta-2,4-dienylidenes [(2_{S-X-C} vs. 2_{T-X-C}), (2_{S-X-Si} vs. 2_{T-X-Si}), (2_{S-X-Ge} vs. 2_{T-X-Ge}), (2_{S-X-Sn} vs. 2_{T-X-Sn}), and (2_{S-X-Pb} vs. 2_{T-X-Pb}), respectively: Series 2], where X = H, F, Cl and Br

Compound(s)	E	H	G	ZPE
2_{S-F-C}	−292.017683	−292.016739	−292.050377	37.08
2_{S-Cl-C}	−652.374691	−652.373747	−652.408780	36.14
2_{S-Br-C}	−2766.295660	−2766.294716	−2766.331118	35.77
2_{T-F-C}	−292.031866	−292.030922	−292.065412	37.20
2_{T-Cl-C}	−652.389988	−652.389044	−652.424873	36.32
2_{T-Br-C}	−2766.310597	−2766.309653	−2766.346851	35.97
2_{S-F-Si}	−543.498301	−543.497356	−543.534410	35.07
$2_{S-Cl-Si}$	−903.848484	−903.847540	−903.885721	34.16
$2_{S-Br-Si}$	−3017.774223	−3017.773279	−3017.813346	33.79
2_{T-F-Si}	−543.468239	−543.467295	−543.503335	35.24
$2_{T-Cl-Si}$	−903.819812	−903.818868	−903.856344	34.47
$2_{T-Br-Si}$	−3017.746433	−3017.745489	−3017.784241	34.05
2_{S-F-Ge}	−2331.017215	−2331.016271	−2331.053966	34.61
$2_{S-Cl-Ge}$	−2691.367931	−2691.366987	−2691.406146	33.75
$2_{S-Br-Ge}$	−4805.293324	−4805.292380	−4805.332831	33.35
2_{T-F-Ge}	−2330.974877	−2330.973933	−2331.012360	33.72
$2_{T-Cl-Ge}$	−2691.336222	−2691.335278	−2691.374968	33.32
$2_{T-Br-Ge}$	−4805.252471	−4805.251527	−4805.291782	33.28
2_{S-F-Sn}	−170.698902	−170.697958	−170.739183	32.98
$2_{S-Cl-Sn}$	−172.482038	−172.481094	−172.520897	33.37
$2_{S-Br-Sn}$	−257.392035	−257.391090	−257.429585	34.17
2_{T-F-Sn}	−170.651897	−170.650953	−170.693228	31.89
$2_{T-Cl-Sn}$	−172.434998	−172.434054	−172.474886	32.31
$2_{T-Br-Sn}$	−257.344060	−257.343116	−257.382550	33.15
2_{S-F-Pb}	−170.794384	−170.793440	−170.835614	32.70
$2_{S-Cl-Pb}$	−172.577378	−172.576434	−172.617184	33.09
$2_{S-Br-Pb}$	−257.487132	−257.486188	−257.525611	33.91
2_{T-F-Pb}	−170.734542	−170.733597	−170.776732	31.57
$2_{T-Cl-Pb}$	−172.516659	−172.515715	−172.557426	31.94
$2_{T-Br-Pb}$	−257.437404	−257.436460	−257.476884	32.84

Table 3
Calculated B3LYP/6-311++G (3df, 2p) bond length (R_1–R_6), bond angles (A_1–A_6), and dihedral angles (D_1–D_6) for M = C, Si, Ge, Sn and Pb in Series 1 (with X = H, F, Cl and Br)
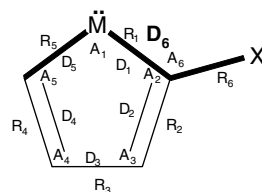
Compound	R_1	R_2	R_3	R_4	R_5	R_6	A_1	A_2	A_3	A_4	A_5	A_6	D_1	D_2	D_3	D_4	D_5	D_6
$1_{S–H–C}$	1.397	1.406	1.461	1.406	1.398	1.077	121.0	94.5	110.2	110.2	94.5	131.2	−32.6	16.4	0.0	−16.4	32.6	169.9
$1_{S–F–C}$	1.436	1.36	1.461	1.46	1.08	1.33	118.7	103.8	100.1	117.3	89.8	123.5	−29.04	7.8	11.6	−25.2	31.6	150.4
$1_{S–Cl–C}$	1.431	1.374	1.542	1.463	1.36	1.706	120.4	101.2	102.9	116.2	89.9	125.4	−30.1	9.3	9.2	−23.2	31.92	147.3
$1_{S–Br–C}$	1.429	1.377	1.451	1.464	1.35	1.863	120.8	100.8	100.3	116.0	89.86	125.6	−30.2	9.6	8.7	−22.7	31.9	146.6
$1_{T–H–C}$	1.439	1.355	1.451	1.355	1.439	1.079	111.8	103.9	110.1	110.1	103.9	127.0	0.04	0.0	0.0	0.0	0.0	180.0
$1_{T–F–C}$	1.438	1.333	1.479	1.394	1.389	1.329	112	109.7	106.2	110.6	103.4	123	1.6	−0.04	−1.5	2.4	−2.4	−176.2
$1_{T–Cl–C}$	1.482	1.325	1.463	1.372	1.418	1.713	109.5	106.8	107.9	111.3	104.3	124	−3.1	1.0	1.4	−3.2	3.8	174.7
$1_{T–Br–C}$	1.454	1.346	1.456	1.384	1.385	1.866	112.6	105.1	108.0	110.7	103.5	124.8	−1.7	1.6	−1.1	0.0	1	177.3
$1_{S–H–Si}$	1.925	1.344	1.499	1.344	1.926	1.08	87.5	109.9	115.7	115.7	109.9	127.5	0.0	0.0	0.0	0.0	0.0	180.0
$1_{S–F–Si}$	1.970	1.335	1.493	1.350	1.904	1.355	85.1	113.3	112.3	117.4	111.9	124.2	0.0	0.0	0.0	0.0	0.0	180.0
$1_{S–Cl–Si}$	1.965	1.339	1.492	1.348	1.909	1.748	85.8	112.2	113.4	117.1	111.5	124.5	0.0	0.0	0.0	0.0	0.0	180.0
$1_{S–Br–Si}$	1.963	1.339	1.494	1.348	1.911	1.905	85.9	112.2	113.5	117.0	111.5	124.6	0.0	0.0	0.0	0.0	0.0	180.0
$1_{T–H–Si}$	1.838	1.367	1.465	1.367	1.837	1.08	96.27	104.1	117.8	117.8	104.1	131.3	0.0	0.0	0.0	0.0	0.0	180.0
$1_{T–F–Si}$	1.970	1.335	1.492	1.351	1.904	1.355	85.1	113.3	112.3	117.4	111.9	124.3	0.0	0.0	0.0	0.0	0.0	180.0
$1_{T–Cl–Si}$	1.857	1.361	1.462	1.370	1.832	1.738	95.1	105.5	116.2	118.8	104.5	129.8	0.0	0.0	0.0	0.0	0.0	180.0
$1_{T–Br–Si}$	1.854	1.362	1.463	1.369	1.832	1.894	95.2	105.4	116.2	118.7	104.4	129.9	0.0	0.0	0.0	0.0	0.0	180.0
$1_{S–H–Ge}$	1.917	1.316	1.518	1.316	1.916	1.08	86.0	112.3	114.7	114.6	112.4	126.8	0.0	0.0	0.0	0.0	0.0	180.0
$1_{S–F–Ge}$	2.068	1.334	1.489	1.349	2.001	1.355	82.4	113.0	113.9	118.9	111.8	124.8	0.0	0.0	0.0	0.0	0.0	180.0
$1_{S–Cl–Ge}$	2.063	1.338	1.489	1.347	2.003	1.749	83.1	112.0	114.9	118.6	111.5	125.0	0.0	0.0	0.0	0.0	0.0	180.0
$1_{S–Br–Ge}$	2.062	1.338	1.492	1.346	2.007	1.908	83.2	112.0	115.0	118.5	111.4	125.1	0.0	0.0	0.0	0.0	0.0	180.0
$1_{T–H–Ge}$	1.871	1.474	1.336	1.474	1.872	1.08	85.2	113.4	113.9	114.0	113.3	129.2	0.0	0.0	0.0	0.0	0.0	180.0
$1_{T–F–Ge}$	2.010	1.429	1.386	1.425	2.007	1.342	79.3	116.3	113.4	115.4	115.5	127.3	0.0	0.0	0.0	0.0	0.0	180.0
$1_{T–Cl–Ge}$	2.011	1.435	1.385	1.423	2.004	1.731	80.3	115.0	114.0	115.8	114.8	127.0	0.0	0.0	0.0	0.0	0.0	180.0
$1_{T–Br–Ge}$	2.012	1.434	1.387	1.424	2.003	1.887	80.4	115.0	114.1	115.8	114.7	127.1	0.0	0.0	0.0	0.0	0.0	180.0
$1_{S–H–Sn}$	2.203	1.343	1.494	1.343	2.203	1.09	80.0	110.3	119.8	119.8	110.3	129.3	0.0	0.0	0.0	0.0	0.0	180.0
$1_{S–F–Sn}$	2.241	1.337	1.486	1.349	2.182	1.364	78.1	112.5	116.6	121.3	111.5	126.9	0.0	0.0	0.0	0.0	0.0	180.0
$1_{S–Cl–Sn}$	2.121	1.217	1.366	1.229	2.062	1.244	78.0	112.4	116.5	121.2	111.4	126.8	0.0	0.0	0.0	0.0	0	180
$1_{S–Br–Sn}$	2.232	1.340	1.488	1.347	2.188	1.920	78.8	111.5	117.7	121.0	110.9	126.9	0.0	0.0	0.0	0.0	0.0	180.0

1_{T-H-Sn}	2.187	1.434	1.385	1.432	1.09	2.187	77.0	113.6	117.8	113.7	113.7	129.3	0.0	0.0	0.0	0.0	0.0	180.0
1_{T-F-Sn}	2.206	1.429	1.386	1.425	1.349	2.197	74.8	116.1	115.9	117.7	115.6	129.1	0.0	0.0	0.0	0.0	0.0	180.0
$1_{T-Cl-Sn}$	2.167	1.429	1.378	1.468	1.763	2.156	76.9	115.1	116.7	117.1	113.8	128.7	0.0	0.0	0.0	0.0	0.0	180.0
$1_{T-Br-Sn}$	2.203	1.435	1.386	1.423	1.896	2.190	75.9	114.7	116.5	118.3	114.6	128.6	0.0	0.0	0.0	0.0	0.0	180.0
1_{S-H-Pb}	2.267	1.344	1.492	1.343	1.09	2.266	78.3	110.2	120.6	120.7	110.2	129.7	0.0	0.0	0.0	0.0	0.0	180.0
1_{S-F-Pb}	2.307	1.338	1.484	1.348	1.367	2.246	76.6	112.2	117.6	122.2	111.4	127.6	0.0	0.0	0.0	0.0	0.0	180.0
$1_{S-Cl-Pb}$	2.300	1.340	1.486	1.347	1.758	2.251	77.2	111.5	118.5	122.0	110.9	127.4	0.0	0.0	0.0	0.0	0.0	180.0
$1_{S-Br-Pb}$	2.298	1.340	1.488	1.346	1.925	2.253	77.2	111.4	118.6	121.9	110.9	127.5	0.0	0.0	0.0	0.0	0.0	180.0
1_{T-H-Pb}	2.209	1.346	1.476	1.346	1.079	2.206	84.0	104.6	123.3	123.3	104.7	128.9	0.0	0.0	0.0	0.0	0.0	180.0
1_{T-F-Pb}	2.280	1.428	1.386	1.424	1.353	2.266	73.3	115.8	116.8	118.7	115.4	130.0	0.0	0.0	0.0	0.0	0.0	180.0
$1_{T-Cl-Pb}$	2.276	1.433	1.385	1.424	1.738	2.257	74.3	114.6	117.4	119.0	114.7	129.5	0.0	0.0	0.0	0.0	0.0	180.0
$1_{T-Br-Pb}$	2.271	1.434	1.387	1.424	1.902	2.258	74.4	114.6	117.3	119.2	114.5	129.3	0.0	0.0	0.0	0.0	0.0	180.0

All dihedral angles except D_6 have *cis* geometries.

separations are compared for the group 14 divalent five member cyclic conjugated structures: C_5H_3X, C_4H_3SiX, C_4H_3GeX, C_4H_3SnX, and C_4H_3PbX (X = H, F, Cl, and Br) (Fig. 1, Tables 1,2, and Scheme 3). Depending on the position of X, these 70 divalent structures are divided into two series (Series 1 and 2). Series 1 includes 40 structures with the formulae of 2-X-cyclopenta-2,4-dienylidenes, plus sila-, germa-, stana-, and plumba-2-X-cyclopenta-2,4-dienylidenes [(1_{S-X-C} vs. 1_{T-X-C}), (1_{S-X-Si} vs. 1_{T-X-S}), (1_{S-X-Ge} vs. 1_{T-X-Ge}) (1_{S-X-Sn} vs. 1_{T-X-Sn}), and (1_{S-X-Pb} vs. 1_{T-X-Pb}), respectively]. Series 2 includes 30 structures with the formulae of 3-X-cyclopenta-2,4-dienylidenes, plus sila-, germa-, stana-, and plumba-3-X-cyclopenta-2,4-dienylidenes [(2_{S-X-C} vs. 2_{T-X-C}), (2_{S-X-Si} vs. 2_{T-X-Si}), (2_{S-X-Ge} vs. 2_{T-X-Ge}), (2_{S-X-Sn} vs. 2_{T-X-Sn}) and (2_{S-X-Pb} vs. 2_{T-X-Pb}), respectively]. The 10 structures which have X = H are included in Series 1.

B3LYP calculated energies (E), enthalpies (H) and free energies (G) for Series 1 and 2 are reported (Tables 1 and 2, respectively). Geometrical parameters including bond length ($R_1–R_6$), bond angles ($A_1–A_6$), and dihedral angles ($D_1–D_6$) for Series 1 and 2 are calculated at B3LYP/6-311++G (3df, 2p) level (Tables 3 and 4). Sum of electronic and thermal energy differences between singlet and triplet states, $\Delta E_{(t-s)}$; sum of electronic and thermal enthalpy differences between singlet and triplet states, $\Delta H_{(t-s)}$; sum of electronic and thermal free energy differences between singlet and triplet states, $\Delta G_{(t-s)}$, are calculated for Series 1 and 2, at B3LYP/6-311++G (3df, 2p) (Table 5).

Singlet states of carbenes 1_{S-X-C} and 2_{S-X-C}, appear non-planar while their corresponding triplet states 1_{T-X-C} and 2_{T-X-C} are both planar and more stable (Tables 1–4). In contrast, their analogous silylenes, germylenes, stanylenes and plumbylenes in both singlet and triplet states have planar structures with the singlet states being more stable than their corresponding triplet states. The question of "why the employed carbenes are ground state triplets while silylenes, germylenes, stanylenes and plumbylenes are ground state singlets" is well explained in the recent works of Apeloig and West [27].

The energies of HOMO and LUMO orbitals, for both Series 1 and 2, are obtained via NBO analysis (Fig. 2) [28]. UB3LYP/6-311++G(3df, 2p) calculated energy difference between HOMO and LUMO of singlet (stable) states, $\Delta_{(LUMO-HOMO)}$, for divalent elements, M = Si, Ge, Sn and Pb appear to have linear relationships with $\Delta G_{(t-s)}$; showing correlation coefficient (R^2) values of 0.89, 0.94, 0.93 and 0.95 for silylenes, germylenes, stanylenes and plumbylenes, respectively.

For M = Si, similar ΔG_{t-s} are found for 2- or 3-halogenated derivatives. In contrast, 3-halo-substituted species have higher ΔG_{t-s}, when M = Pb, Sn and Ge;

Table 4
Calculated B3LYP/6-311++G (3df,2p) bond length (R_1–R_6), bond angles (A_1–A_6), and dihedral angles (D_1–D_6) for M = C, Si, Ge, Sn and Pb in Series 2 (with X = F, Cl and Br)
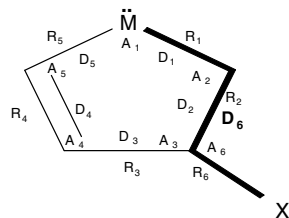
Compound	R_1	R_2	R_3	R_4	R_5	R_6	A_1	A_2	A_3	A_4	A_5	A_6	D_1	D_2	D_3	D_4	D_5	D_6
$2_{S–F–C}$	1.359	1.466	1.466	1.378	1.443	1.08	118.2	92.2	115.8	103.7	100.7	131.6	−30.6	18.7	−2.3	−14.7	32.2	−171.7
$2_{S–Cl–C}$	1.35	1.46	1.451	1.377	1.439	1.725	120.2	92.6	115.0	104.8	99.8	118.7	−30.4	19.0	−3.9	−12.7	30.9	−131.8
$2_{S–Br–C}$	1.346	1.464	1.453	1.377	1.438	1.89	121.3	91.1	115.2	104.6	99.6	118.0	−29.6	18.4	−3.9	−12.1	30.1	−129.6
$2_{T–F–C}$	1.386	1.392	1.465	1.359	1.459	1.338	113.2	102.7	111.9	106.8	105.4	126.2	0.0	0.0	0.0	0.0	0.0	180.0
$2_{T–Cl–C}$	1.383	1.386	1.453	1.354	1.467	1.707	112.6	103.6	111.0	108.1	104.6	126.3	0.0	0.0	0.0	0.0	0.0	180.0
$2_{T–Br–C}$	1.386	1.393	1.452	1.353	1.46	1.86	112.8	102.8	111.6	107.4	105.2	125.5	0.0	0.0	0.0	0.0	0.0	180.0
$2_{S–F–Si}$	1.898	1.338	1.494	1.336	1.960	1.348	87.9	109.0	119.4	113.3	110.5	125.1	0.0	0.0	0.0	0.0	0.0	180.0
$2_{S–Cl–Si}$	1.911	1.339	1.502	1.338	1.944	1.758	87.8	109.5	118.1	113.8	110.9	125.3	0.0	0.0	0.0	0.0	0.0	180.0
$2_{S–Br–Si}$	1.915	1.337	1.502	1.337	1.942	1.922	87.8	109.2	118.3	113.8	110.9	125.2	0.0	0.0	0.0	0.0	0.0	180.0
$2_{T–F–Si}$	1.792	1.365	1.516	1.320	1.820	1.357	95.0	106.5	115.6	115.0	107.8	125.5	0.0	0.0	0.0	0.0	0.0	180.0
$2_{T–Cl–Si}$	1.831	1.363	1.462	1.369	1.840	1.757	96.5	103.3	119.3	116.6	104.4	122.9	0.0	0.0	0.0	0.0	0.0	180.0
$2_{T–Br–Si}$	1.833	1.362	1.462	1.365	1.840	1.917	96.6	103.1	119.4	116.5	104.4	122.7	0.0	0.0	0.0	0.0	0.0	180.0
$2_{S–F–Ge}$	1.993	1.336	1.491	1.334	2.058	1.354	85.2	108.8	121.0	114.9	110.2	124.3	0.0	0.0	0.0	0.0	0.0	180.0
$2_{S–Cl–Ge}$	2.009	1.336	1.499	1.335	2.041	1.766	85.0	109.2	119.7	115.3	110.6	124.4	0.0	0.0	0.0	0.0	0.0	180.0
$2_{S–Br–Ge}$	2.013	1.335	1.499	1.337	2.039	1.931	85.1	109.0	119.9	115.4	110.6	124.3	0.0	0.0	0.0	0.0	0.0	180.0
$2_{T–F–Ge}$	2.014	1.420	1.383	1.425	1.995	1.350	81.9	111.6	118.5	113.4	114.6	121.2	0.0	0.0	0.0	0.0	0.0	180.0
$2_{T–Cl–Ge}$	2.009	1.427	1.388	1.421	1.994	1.752	81.8	112.3	117.1	114.2	114.5	122.0	0.0	0.0	0.0	0.0	0.0	180.0
$2_{T–Br–Ge}$	1.934	1.353	1.464	1.358	1.938	1.924	92.8	103.3	121.2	118.2	104.6	121.8	0.0	0.0	0.0	0.0	0.0	180.0
$2_{S–F–Sn}$	2.176	1.335	1.489	1.338	2.227	1.364	80.5	108.6	123.3	117.7	109.8	123.3	0.0	0.0	0.0	0.0	0.0	180.0
$2_{S–Cl–Sn}$	2.191	1.336	1.496	1.338	2.213	1.083	80.3	109.0	122.3	118.1	110.4	123.3	0.0	0.0	0.0	0.0	0.0	180.0
$2_{S–Br–Sn}$	2.195	1.334	1.497	1.340	2.210	1.949	80.3	108.8	122.4	118.1	110.4	123.2	0.0	0.0	0.0	0.0	0.0	180.0
$2_{T–F–Sn}$	2.204	1.420	1.386	1.425	2.184	1.356	77.1	111.6	120.9	115.9	114.5	120.2	0.0	0.0	0.0	0.0	0.0	180.0
$2_{T–Cl–Sn}$	2.198	1.427	1.388	1.422	2.183	1.756	77.0	112.3	119.6	116.6	114.5	120.9	0.0	0.0	0.0	0.0	0.0	180.0
$2_{T–Br–Sn}$	2.200	1.425	1.390	1.422	2.182	1.928	77.1	112.2	119.6	116.6	114.5	121.1	0.0	0.0	0.0	0.0	0.0	180.0
$2_{S–F–Pb}$	2.244	1.334	1.487	1.338	2.290	1.369	79.0	108.2	124.4	118.7	109.7	122.8	0.0	0.0	0.0	0.0	0.0	180.0
$2_{S–Cl–Pb}$	2.260	1.333	1.494	1.339	2.276	1.783	78.7	108.7	123.3	118.9	110.3	122.8	0.0	0.0	0.0	0.0	0.0	180.0
$2_{S–Br–Pb}$	2.266	1.332	1.495	1.339	2.272	1.962	78.8	108.4	123.6	118.9	110.4	122.6	0.0	0.0	0.0	0.0	0.0	180.0
$2_{T–F–Pb}$	2.274	1.419	1.384	1.424	2.253	1.361	75.6	111.4	121.8	116.8	114.4	119.9	0.0	0.0	0.0	0.0	0.0	180.0
$2_{T–Cl–Pb}$	2.200	1.342	1.468	1.346	2.215	1.775	84.2	104.6	124.4	123.0	104.3	121.1	0.0	0.0	0.0	0.0	0.0	180.0
$2_{T–Br–Pb}$	2.210	1.399	1.468	1.347	2.209	1.951	84.2	103.6	125.1	122.5	104.7	120.2	0.0	0.0	0.0	0.0	0.0	180.0

All dihedral angels except D_6 have *cis* geometries.

Table 5
Sum of electronic and thermal energy differences between singlet and triplet states, $\Delta E_{(t-s)}$; sum of electronic and thermal enthalpy differences between singlet and triplet states, $\Delta H_{(t-s)}$; sum of electronic and thermal free energy differences between singlet and triplet states, $\Delta G_{(t-s)}$, for Series 1 and Series 2, calculated at B3LYP/6-311++G (3df, 2p)

Series 1				Series 2			
	$\Delta E_{(t-s)}$	$\Delta H_{(t-s)}$	$\Delta G_{(t-s)}$		$\Delta E_{(t-s)}$	$\Delta H_{(t-s)}$	$\Delta G_{(t-s)}$
1_{H-C}	−8.36	−8.36	−9.20	2_{H-C}	−8.36	−8.36	−9.20
1_{F-C}	−10.73	−10.73	−11.42	2_{F-C}	−8.80	−8.80	−9.33
1_{Cl-C}	−10.31	−10.31	−10.95	2_{Cl-C}	−9.43	−9.43	−9.93
1_{Br-C}	−10.10	−10.10	−10.74	2_{Br-C}	−9.20	−9.20	−9.70
1_{H-Si}	21.33	21.33	20.91	2_{H-Si}	21.33	21.33	20.91
1_{F-Si}	18.99	18.99	19.39	2_{F-Si}	19.02	19.02	19.65
1_{Cl-Si}	18.26	18.26	18.70	2_{Cl-Si}	17.84	17.84	18.55
1_{Br-Si}	18.16	18.16	18.64	2_{Br-Si}	17.67	17.67	18.49
1_{H-Ge}	23.89	23.88	23.41	2_{H-Ge}	23.89	23.88	23.41
1_{F-Ge}	18.68	18.68	18.38	2_{F-Ge}	25.77	25.77	25.31
1_{Cl-Ge}	19.52	19.52	19.18	2_{Cl-Ge}	25.04	25.04	24.53
1_{Br-Ge}	19.78	19.78	19.45	2_{Br-Ge}	25.58	25.58	25.70
1_{H-Sn}	26.86	26.86	26.17	2_{H-Sn}	26.86	26.86	26.17
1_{F-Sn}	22.55	22.55	22.11	2_{F-Sn}	29.20	29.20	28.61
1_{Cl-Sn}	22.62	22.62	22.35	2_{Cl-Sn}	28.57	28.57	27.93
1_{Br-Sn}	23.74	23.74	23.21	2_{Br-Sn}	28.53	28.53	27.87
1_{H-Pb}	33.32	33.32	32.94	2_{H-Pb}	33.32	33.32	32.94
1_{F-Pb}	23.87	23.87	23.38	2_{F-Pb}	30.25	30.25	29.62
1_{Cl-Pb}	24.96	24.96	24.42	2_{Cl-Pb}	37.08	37.08	36.48
1_{Br-Pb}	25.13	25.13	24.57	2_{Br-Pb}	36.55	36.55	35.95

enes > germylenes > silylenes. Such an order is another evidence for the stabilization of the singlet states by the larger valence orbitals [29]. Thus, plumbylenes with the largest valence orbitals and R_1 (Tables 3 and 4) have more stable singlet states, and consequently a larger $\Delta G_{(t-s)}$. Electronic and thermal free energy differences between singlet and triplet states ($\Delta G_{(t-s)}$) have greater values for Series 2 (Fig. 3 and Table 5).

Substitution of hydrogen with halogen in Series 1, in contrast to Series 2, causes a decrease in $\Delta G_{(t-s)}$ (Table 5). Due to the higher electro-negativity of fluorine, when X = F singlet states of Series 2 are more stabilized than their corresponding singlet states in Series 1, for M = C, Si, Ge, Sn and Pb (Tables 1,2). However, triplet states of Series 1 are more stabilized than their corresponding Series 2 isomers, if X = F, when M = Ge, Sn, and Pb. Nevertheless, in cases where M = C and Si, the observation is opposite to the above. For the less electronegative chlorine, where X = Cl, again singlet states of Series 2 are more stabilized than their corresponding singlet states in Series 1, for M = C, Si, Ge, Sn, and Pb (Tables 1,2). However, triplet states of Series 1 are more stabilized than their corresponding Series 2 isomers, if X = Cl, when M = Ge, Sn and Pb. Nevertheless, in cases where M = C and Si, the observation is opposite to the above. Generally the energy gap created by introducing X is larger between singlet states in comparison to their corresponding gap of triplet states.

In order to confirm global minima, for Series 1 and 2, energy surface studies are necessary, since puckering of cyclopenta-2,4-dienylidene rings may alter positions of the global minima. Puckering energy are presented for

and lower ΔG_{t-s}, when M = C. The order of energy differences between X-singlet and the corresponding X-triplet, $\Delta G_{(t-s)}$, for both Series is: plumbylenes > stanyl-
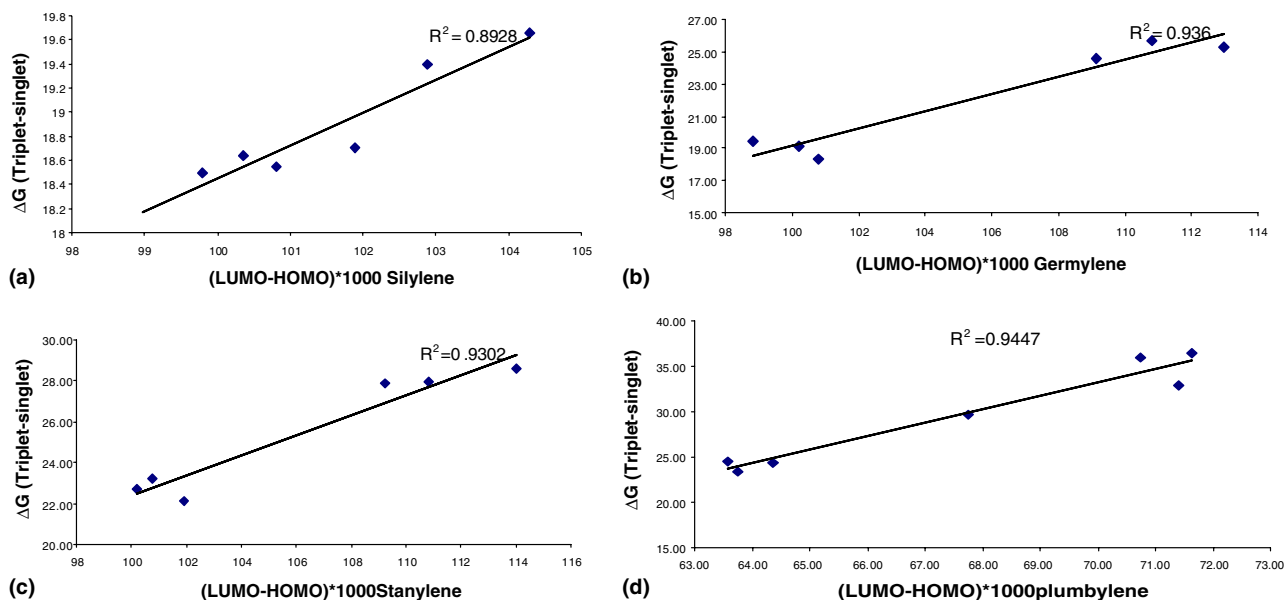

Fig. 2. Linear relationships between singlet LUMO–HOMO energy gaps, and their corresponding singlet–triplet energy separations ($\Delta G_{(t-s)}$), for conjugated, 2- or 3-halogenated five-membered-ring: silylenes (a), germylenes (b), stanylenes (c), plumbylenes (d); with correlation factors (and slopes shown in parenthesis): 0.89 (0.28), 0.94 (0.53), 0.93 (0.49) and 0.95 (1.48), respectively.
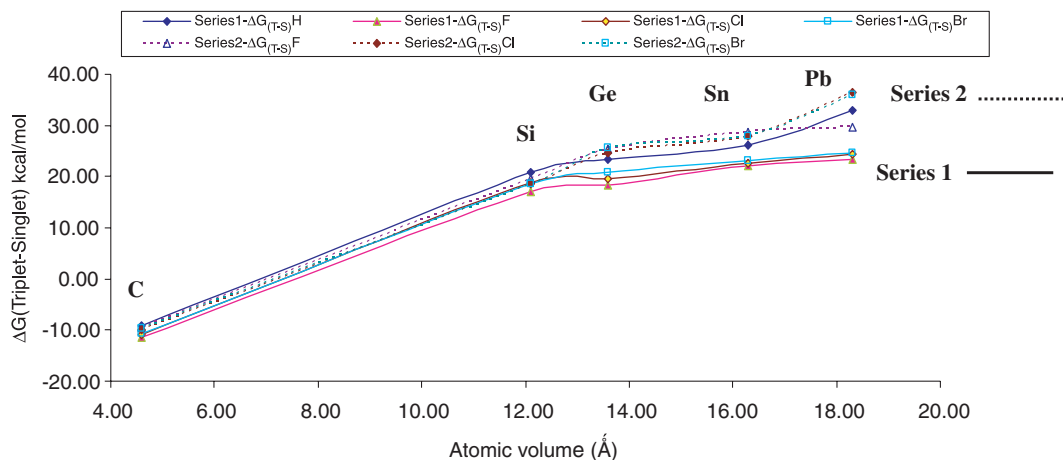
Fig. 3. ΔG (triplet–singlet) vs. atomic volume for carbenes (C), silylenes (Si), germylenes (Ge), stanylenes (Sn), and plumbylenes (Pb) for Series 1 (—): 2-X-cyclopenta-2,4-dienylidenes, together with sila-, germa-, stana-, and plumba-2-X-cyclopenta-2,4-dienylidenes and Series 2 (---): 3-X-cyclopenta-2,4-dienylidenes, plus sila-, germa-, stana-, and plumba-3-X-cyclopenta-2,4-dienylidenes; for X = H, F, Cl and Br.

Series 1 structures (which include 2-X-M-cyclopenta-2,4-dienylidene rings) as a function of dihedral angle D_1 (for M = C, Si, Ge, Sn and Pb) (Fig. 4; Tables 3 and 4). The puckering energy appears higher for triplet states than their corresponding singlet states. Puckering only alters the position of the global minima of singlet carbenes (M = C). Singlet states of carbenes have two non-planar minima, a global and a local minimum (Fig. 4). Moreover, puckering energy surfaces are sketched for both singlet (a) and triplet (b) states of 2-X-geracyclopenta-2,4-dienylidene rings as a function of dihedral angle D_1 (Fig. 5). The order of puckering energy barriers for both singlet and triplet states is: carb-

enes > silylenes > germylenes > stanylenes > plumbylenes. Nevertheless, the puckering energy barriers are higher for triplet states compared to their corresponding singlet states. Puckering energy surface for Series 2 is similar to that of Series 1. For the sake of brevity, the latter energy surface is excluded, and data pertaining to $\angle$C–M–C angles (A_1) larger than 25° are omitted.

Generally every singlet 3-halo-substituted entry in Series 2 has a larger $\angle$C–M–C angle (A_1) than the corresponding singlet 2-halo-substituted isomer in Series 1. Similar order exists for triplet states.

Interestingly, $\angle$C–M–C angles (A_1), in singlet states, are larger than their corresponding $\angle$C–M–C angles
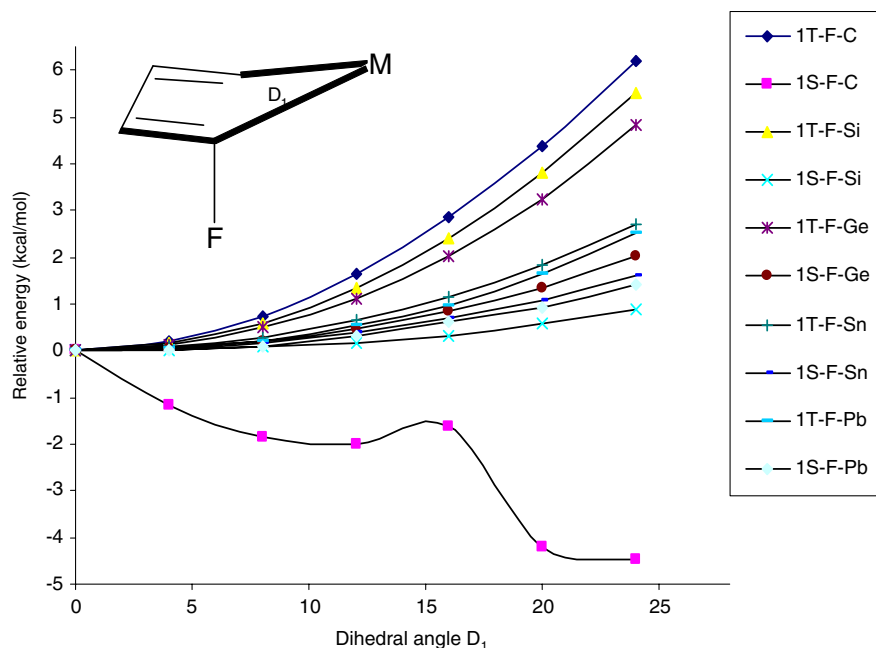

Fig. 4. Puckering energy of 2-X-M-cyclopenta-2,4-dienylidene rings as a function of dihedral angle D_1 for M = C, Si, Ge, Sn and Pb (where X = F).
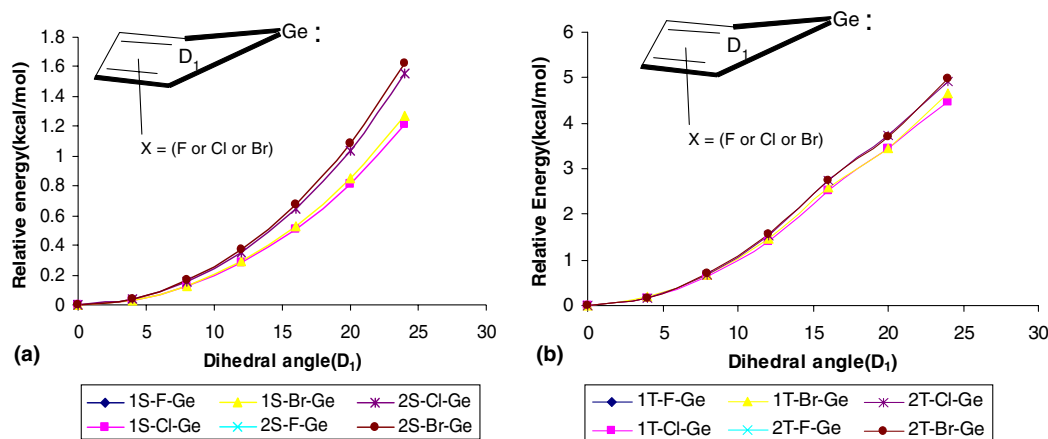
Fig. 5. Puckering energy for both singlet (a) and triplet (b) states of 2-X-geracyclopenta-2,4-dienylidene rings as a function of dihedral angle D_1 for X = F.
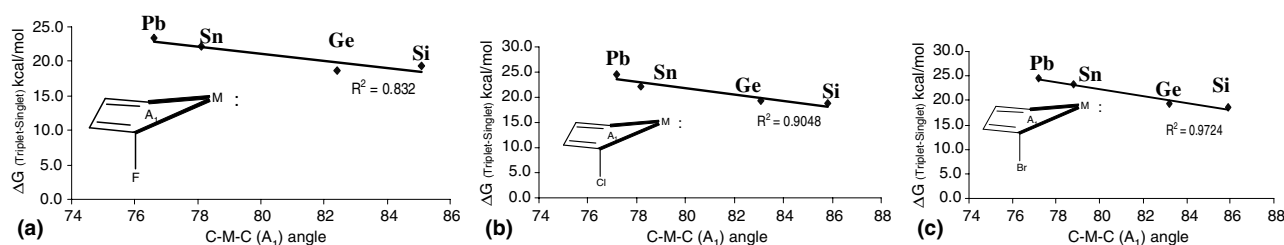

Fig. 6. Correlations between $\Delta G_{(triplet–singlet)}$ and the $\angle$C–M–C angle (A_1) for M = C, Si, Ge, Sn and Pb in Series 1 (R^2 = correlation coefficient; X = F, Cl and Br).

(A_1) in triplet states, most likely due the higher aromaticity of the singlet 2-X-M-cyclopenta-2,4-dienylidene rings, compared to corresponding triplet state (Tables 3 and 4). Regardless of the multiplicity, the smaller is A_1, the larger is $\Delta G_{(t–s)}$. Linear correlations are found between $\Delta G_{(t–s)}$ and A_1, for both Series 1 and 2, with acceptable correlation coefficients (R) (Fig. 6). The trend of R^2 follows electro-positivity: bromine (0.97) > chlorine (0.90) > fluorine (0.83). Moreover, linear relationships between $\Delta G_{(t–s)}$ vs. $\Delta_{(LUMO–HOMO)}$ and $\Delta G_{(t–s)}$ vs. A_1 are found. Consequently one can expect a linear relation between $\Delta_{(LUMO–HOMO)}$ and angle A_1.

Three dimensional iso-surface HOMO plots obtained for triplet as well as singlet silylenes, and their heavier analogs, at UB3LYP/6-311++G** level of theory illustrate the σ^2 ($^1A_1$) configuration for HOMO of the singlet species of silylenes, germylenes, stanylenes and polombylenes (Fig. 7).

The benchmark calculations are done and compared for :CH$_2$, :SiH$_2$, :GeH$_2$, :SnH$_2$ and :PbH$_2$. Absolute energies, molecular geometries, triplet–singlet energy gaps are reported in Tables 6–8, respectively. Triplet states in these simplest studied compounds have greater $\angle$C–M–C angles than those of singlet state.

In order to perform solvation analysis of structures in Series 1 and 2, their optimizations are carried out in chloroform, using the "Polarizable Continuum Solvation Model" (PCSM) [26,27]. The physical properties of the systems, such as free energies, electrostatic and non-electrostatic interaction are found (Table 9). The non-electrostatic interactions include cavitations, dispersion and repulsion energies. These compounds show positive ΔG_{sol}, indicating their inability of dissolving in choloroform. It was found that in polar solvents, singlet–triplet gaps increase for M = Si, Ge, Sn and Pb, due to stabilizing electrostatic interactions between the solvent and the charge distribution of the singlet [29]. Further analysis of structures in Series 1 and 2 awaits completion of our investigation.

4. Conclusion

Singlet states of carbens $1_{S–X–C}$ and $2_{S–X–C}$, appear non-planar while their corresponding triplet states $1_{T–X–C}$ and $2_{T–X–C}$ are both planar and more stable. In contrast, their analogous silylenes, germylenes, stanylenes and plumbylenes in both singlet and triplet states have

(a) 1_{T-H-Si} (β electrons)

(b) 1_{T-H-Si} (α electrons)

(c) 1_{T-H-Ge} (β electrons)

(d) 1_{T-H-Ge} (α electrons)

(e) 1_{S-H-Si} (α, β electrons)
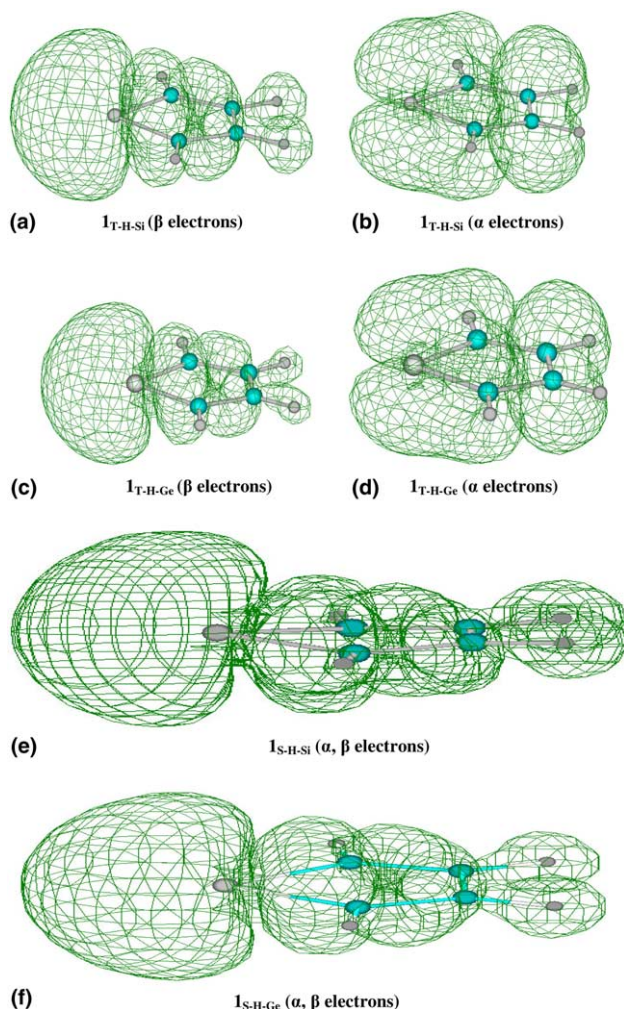
(f) 1_{S-H-Ge} (α, β electrons)

Fig. 7. Three dimensional iso-surface HOMO plots are shown for triplet silylene (a,b), germylene (c,d), singlet silylenes (e), and singlet germylene (f) at UB3LYP/6-311++G** level of theory.

Table 7
Calculated B3LYP/6-311++G (3df, 2p) bond length (R_1, R_2), bond angles (A_1) of :MH$_2$, where M = C, Si, Ge, Sn and Pb

$$\overset{\displaystyle ..}{R_1-\underset{\underset{\textstyle H}{A_1}}{M}-R_2}$$

Compound(s)	R_1	R_2	A_1
:CH$_2$ singlet	1.114	1.113	101.5
:CH$_2$ triplet	1.080	1.080	135.4
:SiH$_2$ singlet	1.527	1.527	91.5
:SiH$_2$ triplet	1.488	1.488	118.7
:GeH$_2$ singlet	1.597	1.596	90.8
:GeH$_2$ triplet	1.546	1.546	119.8
:SnH$_2$ singlet	1.784	1.784	90.3
:SnH$_2$ triplet	1.727	1.727	117.6
:PbH$_2$ singlet	1.830	1.830	90.0
:PbH$_2$ triplet	1.777	1.778	119.3

Table 8
Energy difference between singlet and their corresponding triplet states: sum of electronic and thermal energies, $\Delta E_{(t-s)}$; sum of electronic and thermal enthalpies, $\Delta H_{(t-s)}$; sum of electronic and thermal free energies, $\Delta G_{(t-s)}$, for :MH$_2$ where M = C, Si, Ge, Sn and Pb

:MH$_2$	Others calculations (kcal mol^{-1})	Our calculations (kcal mol^{-1})		
		$\Delta E_{(t-s)}$	$\Delta H_{(t-s)}$	$\Delta G_{(t-s)}$
:CH$_2$	−9.0[a]	−11.39	−11.39	−11.82
:SiH$_2$	21[a]	20.63	20.63	20.08
:GeH$_2$	23[a]	27.07	27.07	26.54
:SnH$_2$	23–24[b]	26.10	26.10	25.54
:PbH$_2$	No report accordance to our knowledge	36.66	36.66	36.10

[a] See reference [5a].
[b] See reference [30].

planar structures with the singlet states being more stable than their corresponding triplet states.

Every 3-halo-substituted entry in Series 2 is more stable than the corresponding 2-halo-substituted isomer in Series 1. The order of energy difference between X-singlet and the corresponding X-triplet, $\Delta G_{(t-s)}$, for both
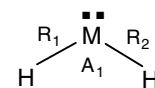
Series is: plumbylenes > stanylenes > germylenes > silylenes. This order is more pronounced for Series 2.

We found linear relations between $\Delta G_{(t-s)}$ vs. $\Delta_{(LUMO-HOMO)}$ and $\Delta G_{(t-s)}$ vs. A_1. Consequently we can expect that a linear relation does exist between $\Delta_{(LUMO-HOMO)}$ and the angle A_1.

Table 6
Calculated B3LYP/6-311++G(3df, 2p) sum of electronic and thermal energies (*E*), sum of electronic and thermal enthalpies (*H*), sum of electronic and thermal Gibbs free energies (*G*) and zero-point energies (ZPE) for singlet and triplet states of :MH$_2$, where M = C, Si, Ge, Sn and Pb

Compound(s)	E	H	G	ZPE
:CH$_2$ singlet	−39.1274000	−39.1264560	−39.1485860	10.36
:CH$_2$ triplet	−39.1461160	−39.1451720	−39.1679850	10.75
:SiH$_2$ singlet	−290.6260190	−290.6250750	−290.6492820	7.30
:SiH$_2$ triplet	−290.5934710	−290.5925270	−290.6176090	7.53
:GeH$_2$ singlet	−2078.1460220	−2078.1450770	−2078.1707710	6.75
:GeH$_2$ triplet	−2078.1032900	−2078.1023460	−2078.1288920	7.04
:SnH$_2$ singlet	−4.5116310	−4.5106870	−4.5373850	6.03
:SnH$_2$ triplet	−4.4701890	−4.4692450	−4.4968370	6.14
:PbH$_2$ singlet	−4.6118910	−4.6109470	−4.6385380	5.72
:PbH$_2$ triplet	−4.5532000	−4.5522560	−4.5807420	5.53

Table 9
B3LYP/6-311++G (3df, 2p) solvation analysis data for structures in Series 1 and 2, in chloroform, using the "Polarizable Continuum Solvation Model" (PCSM)

Compound	Total electrostatic	Total non-electrostatic			ΔG (solvation)
		Capitation energy	Dispersion energy	Repulsion energy	
1_{S-H-CB}	−1.94	7.23	−10.28	2.68	−2.3
1_{S-F-CB}	−1.14	8.7	−9.35	1.45	−0.33
2_{S-F-CB}	−1.95	8.55	−9.83	1.93	−1.3
$1_{S-Cl-CB}$	−0.97	9.71	−10.17	1.45	0.03
$2_{S-Cl-CB}$	−1.85	9.63	−10.72	1.96	−0.98
$1_{S-Br-CB}$	−0.9	10.05	−10.77	1.52	−0.09
$2_{S-Br-CB}$	−1.97	9.99	−11.34	2.05	−1.27
1_{T-H-CB}	−0.73	7.74	−8.93	1.48	−0.45
1_{T-F-CB}	−1.15	8.56	−9.73	1.76	−0.55
2_{T-F-CB}	−0.78	8.73	−9.39	1.47	0.02
$1_{T-Cl-CB}$	−0.79	9.76	−10.31	1.5	0.16
$2_{T-Cl-CB}$	−0.66	9.72	−10.23	1.47	0.3
$1_{T-Br-CB}$	−0.77	10.09	−10.95	1.58	−0.05
$2_{T-Br-CB}$	−0.7	10.08	−10.83	1.54	0.09
$1_{S-H-SiB}$	−1.82	8.04	−7.84	1.41	−0.21
$1_{S-F-SiB}$	−3.44	8.99	−8.41	1.39	−1.48
$2_{S-F-SiB}$	−2.61	8.96	−8.25	1.33	−0.57
$1_{S-Cl-SiB}$	−3	10.11	−9.37	1.4	−0.86
$2_{S-Cl-SiB}$	−3.56	10.03	−9.1	1.33	−1.31
$1_{S-Br-SiB}$	−3.75	10.46	−9.99	1.48	−1.81
$2_{S-Br-SiB}$	−3.53	10.39	−9.71	1.39	−1.46
$1_{T-H-SiB}$	−1.67	7.8	−8.46	2.01	−0.32
$1_{T-F-SiB}$	−3.17	8.91	−8.43	1.4	−1.3
$2_{T-F-SiB}$	−4.35	8.9	−8.27	1.34	−2.38
$1_{T-Cl-SiB}$	−3.39	10.03	−9.41	1.41	−1.36
$2_{T-Cl-SiB}$	−4.74	9.96	−9.13	1.33	−2.58
$1_{T-Br-SiB}$	−4.77	10.38	−10.05	1.49	−2.96
$2_{T-Br-SiB}$	−5.12	10.31	−9.73	1.39	−3.15
$1_{S-H-GeB}$	−1.2	8.47	−7.5	1.3	1.08
$1_{S-F-GeB}$	−1.49	9.63	−7.97	1.29	1.45
$2_{S-F-GeB}$	−1.16	9.58	−7.89	1.27	1.8
$1_{S-Cl-GeB}$	−1.28	10.72	−8.95	1.34	1.84
$2_{S-Cl-GeB}$	−0.91	10.64	−8.74	1.26	2.26
$1_{S-Br-GeB}$	−1.31	11.08	−9.58	1.41	1.6
$2_{S-Br-GeB}$	−1.06	11	−9.35	1.33	1.92
$1_{T-H-GeB}$	−2.08	8.29	−8.03	1.82	0
$1_{T-F-GeB}$	−1.42	9.56	−8.24	1.55	1.45
$2_{T-F-GeB}$	−1.18	9.41	−8.43	1.78	1.57
$1_{T-Cl-GeB}$	−1.31	10.63	−9.21	1.61	1.73
$2_{T-Cl-GeB}$	−0.64	10.48	−9.26	1.75	2.34
$1_{T-Br-GeB}$	−1.25	10.98	−9.82	1.67	1.58
$2_{T-Br-GeB}$	−1.14	10.86	−9.41	1.34	1.66
$1_{S-H-SnB}$	−0.85	9.28	−7.26	1.29	2.46
$1_{S-F-SnB}$	−1.62	10.26	−7.73	1.24	2.16
$2_{S-F-SnB}$	−1.45	10.2	−7.67	1.23	2.31
$1_{S-Cl-SnB}$	−1.39	10.5	−8.02	1.20	2.48
$2_{S-Cl-SnB}$	−1.35	11.27	−8.49	1.23	2.65
$1_{S-Br-SnB}$	−1.37	11.69	−9.28	1.36	2.39
$2_{S-Br-SnB}$	−1.4	11.63	−9.1	1.29	2.42
$1_{T-H-SnB}$	−0.93	9.12	−7.75	1.82	2.26
$1_{T-F-SnB}$	−1.03	10.23	−7.96	1.48	2.73
$2_{T-F-SnB}$	−0.96	10.07	−8.16	1.71	2.66
$1_{T-Cl-SnB}$	−0.89	11.25	−8.87	1.5	2.99
$2_{T-Cl-SnB}$	−0.84	11.14	−8.98	1.67	3.01
$1_{T-Br-SnB}$	−0.77	11.61	−9.5	1.61	2.95
$2_{T-Br-SnB}$	−0.84	11.51	−9.59	1.73	2.81

Table 9 (*continued*)

Compound	Total electrostatic	Total non-electrostatic			ΔG (solvation)
		Capitation energy	Dispersion energy	Repulsion energy	
1$_{S–H–PbB}$	−42.31	8.41	−7.81	1.4	−40.31
1$_{S–F–PbB}$	−54.54	9.38	−8.38	1.39	−52.14
2$_{S–F–PbB}$	−44.79	9.35	−8.2	1.33	−42.31
1$_{S–Cl–PbB}$	−52.72	10.5	−9.36	1.41	−50.17
2$_{S–Cl–PbB}$	−45.34	10.4	−9.06	1.33	−42.66
1$_{S–Br–PbB}$	−51.62	10.86	−9.99	1.49	−49.26
2$_{S–Br–PbB}$	−45.2	10.78	−9.69	1.4	−42.7
1$_{T–H–PbB}$	−39.96	8.39	−7.83	1.4	−38.02
1$_{T–F–PbB}$	−41.94	9.18	−8.85	1.92	−39.69
2$_{T–F–PbB}$	−41.94	9.18	−8.85	1.92	−39.69
1$_{T–Cl–PbB}$	−37.39	10.45	−9.67	1.72	−34.88
2$_{T–Cl–PbB}$	−46.75	10.33	−9.09	1.33	−44.17
1$_{T–Br–PbB}$	−39.6	10.81	−10.33	1.79	−37.33
2$_{T–Br–PbB}$	−47.33	10.69	−9.71	1.4	−44.94

Every triplet state has lower tendency (higher barrier) to puckering in comparison to its corresponding singlet state. The order of these tendencies is: carbens < silylenes < germylenes < stanylenes < plumbylenes.

References

[1] P.P. Gaspar, R. West, in: Z. Rappoport, Y. Apeloig (Eds.), Chemistry of Organic Silicon Compounds, vol. 2, Wiley, Chichester, 1997, p. 2436.
[2] (a) M.Z. Kassaee, Z.S. Hossaini, B.N. Haerizade, S.Z. Sayyed-Alangi, J. Mol. Struct.: Theochem. 68 (2004) 129–135;
(b) M.Z. Kassaee, S.Z. Sayyed-Alangi, Z. Hossaini, J. Mol. Struct.: Theochem. 676 (2004) 7–14;
(c) M.Z. Kassaee, Z.S. Hossaini, B.N. Haerizade, S.Z. Sayyed-Alangi, J. Mol. Struct.: Theochem. 68 (2004) 129–135;
(d) M.Z. Kassaee, S.Z. Sayyed-Alangi, Z. Hossaini, J. Mol. Struct.: Theochem. 676 (2004) 7–14;
(e) M.Z. Kassaee, B.N. Haerizade, S. Arshadi, J. Mol. Struct.: Theochem. 639 (2003) 187–193;
(f) M.Z. Kassaee, J. Azarnia, S. Arshadi, J. Mol. Struct.: Theochem. 686 (2004) 115–122.
[3] (a) R. Gleiter, R. Hoffmann, J. Am. Chem. Soc. 90 (1968) 5457;
(b) H. Kollmar, J. Am. Chem. Soc. 100 (1978) 2660;
(c) L. Radom, H.F. Schaefer III, M.A. Vincent, Nouv. J. Chim. 4 (1980) 411;
(d) M. Kausch, H. Durr, J. Chem. Res. 2 (1982).
[4] M.Z. Kassaee, M.R. Nimlos, K.E. Downie, E.E. Waali, Tetrahedron 41 (1985) 1579.

[5] (a) M. Su, S. Chu, Inorg. Chem. 38 (1999) 4819–4823;
(b) A.J. Arduengo, R.L. Harlow, M. Kline, J. Am. Chem. Soc. 113 (1991) 361.
[6] (a) M. Denk, R. Lennon, R. Hayashi, R. West, A. Haaland, H. Belyakov, P. Verne, M. Wagner, N. Metzler, J. Am. Chem. Soc. 116 (1994) 2691;
(b) R. West, M. Denk, Pure Appl. Chem. 68 (1996) 785;
(c) T.A. Schmedake, M. Haaf, Y. Apeloig, T. Müller, S. Bukalov, R. West, J. Am. Chem. Soc. 121 (1999) 9479.
[7] (a) W.A. Herrmann, M. Denk, J. Behm, W. Scherer;, F.R. Klingan, H. Bock, B. Solouki, M. Wagner, Angew. Chem., Int. Ed. Engl. 11 (1992) 1485;
(b) S.B. Choi, P. Bondjouk, Tetrahedron Lett. 41 (2000) 6685–6688.
[8] (a) A. Dhiman, T. Müller, R. West, J.Y. Becker, Organometallics 23 (2004) 5689–5693;
(b) C. Boehme, G. Frenking, J. Am. Chem. Soc. 118 (1996) 2039–2046;
(c) L.A. Leites, S.S. Bukalov, A.V. Zabula, I.A. Garbuzova, D.F. Moser, R. West, J. Am. Chem. Soc. 126 (2004) 4114–4115;
(d) , For divalent but not bi-coordinated stable silicon compounds:P. Jutzi, D. Kanne, C. Krüger, Angew. Chem., Int. Ed. Engl. 25 (1986) 164;
(e) M. Kira, S. Ishida, T. Iwamoto, C. Kabuto, J. Am. Chem. Soc. 121 (1999) 9722;
(f) G.H. Lee, R. West, T. Müller, J. Am. Chem. Soc. 125 (2003) 8114;
(g) , For recent reviews on stable silylenes and germylenes, see:M. Haaf, T.A. Schmedake, R. West, Acc. Chem. Res. 33 (2000) 704.
[9] (a) S.A. Drake, J.M. Standard, R.W. Quandt, J. Phys. Chem. A 106 (2002) 1357–1364;
(b) D.L.S. Brahms, W.P. Dailey, Chem. Rev. 96 (1996) 1585–1632;
(c) J.W. Storer, K.N. Houk, J. Am. Chem. Soc. 115 (1993) 10426–10427.
[10] M.W. Heaven, G.F. Metha, M.A. Buntine, J. Phys. Chem. A 105 (2001) 1185–1196.
[11] (a) M.R. Zachariah, W. Tsang, J. Phys. Chem. 99 (1995) 5308;
(b) D.J. Lucas, L.A. Curtiss, J.A. Pople, J. Chem. Phys. 99 (1993) 6697, and references therein;
(c) P. Boudjouk, E. Black, R. Kumarathasan, Organometallics 10 (1991) 2095.
[12] M.S. Gordon, L.A. Pederson, J. Phys. Chem. 94 (1990) 5527.
[13] P.P. Gaspar, in: M. Jones, R.A. Moss (Eds.), Reactive Intermediates, vol. 1, Wiley-Interscience, New York, 1978, p. 229.

[14] (a) N. Tokitoh, R. Okazaki, Coord. Chem. Rev. 210 (2000) 251;
(b) J. Barrau, G. Rima, Coord. Chem. Rev. 180 (1998) 593.

[15] (a) M.P. Egorov, O.M. Nefedov, T.-S. Lin, P.P. Gaspar, Organometallics 14 (1995) 1539;
(b) D. Bethell, V.D. Parker, Acc. Chem. Res. 21 (1988) 400;
(c) R.N. McDonald, Tetrahedron 45 (1989) 3993.

[16] (a) P.J. Davidson, M.F. Lappert, J. Chem. Soc. Chem. Commun. (1973) 317;
(b) P.J. Davidson, D.H. Harris, M.F. Lappert, J. Chem. Soc. Dalton Trans. (1976) 2268.

[17] N. Kano, K. Shibata, N. Tokitoh, R. Okazaki, Organometallics 18 (1999) 2999.

[18] (a) For reviews, see: E.W. AbelComprehensive Inorganic Chemistry, vol. 2, Pergamon, Oxford, England, 1973, p. 105;
(b) P.G. HarrisonComprehensive organometallic chemistry II, vol. 2, Pergamon, New York, 1995, p. 305;
(c) P.G. HarrisonComprehensive coordination chemistry, vol. 3, Pergamon, Oxford, England, 1987, p. 185;
(d) J. Parr, Polyhedron 16 (1997) 551.

[19] (a) N. Tokitoh, M. Saito, R. Okazaki, J. Am. Chem. Soc. 115 (1993) 2065;
(b) N. Tokitoh, Y. Matsuhashi, R. Okazaki, J. Chem. Soc., Chem. Commun. (1993) 407;
(c) N. Tokitoh, H. Suzuki, R. Okazaki, K. Ogawa, J. Am. Chem. Soc. 115 (1993) 10428.

[20] H. Dfirr, F. Werndorff, Angew. Chem., Int. Ed. 13 (1974) 483.

[21] C. Lee, W. Yang, R.G. Parr, Phys. Rev. B 37 (1988) 785.

[22] A.D. Becke, J. Chem. Phys. 98 (1993) 5648.

[23] M.J. Frisch, G.W. Trucks, H.B. Schlegel, G.E. Scuseria, M.A. Robb, J.R. Cheeseman, V.G. Znkrzewski, G.A. Montgomery, R.E. Startmann, J.C. Burant, S. Dapprich, J.M. Millam, A.D. Daniels, K.N. Kudin, M.C. Strain, O. Farkas, J. Tomasi, V. Barone, M. Cossi, R. Cammi, B. Mennucci, C. Pamelli, G. Adamo, S. Clifford, J. Ochterski, G.A. Petersson, P.Y. Ayala, Q. Cui, K. Morokoma, D.K. Malick, A.D. Rubuck, K. Raghavachari, J.B. Foresman, J. Cioslawski, J.V. Oritz, B.B. Stlefanov, G. Liu, A. Liashenko, P. Piskorz, I. Komaromi, R. Comperts, R.L. Martin, P.J. Fox, T. Keith, M.A. Al-laham, C.Y. Peng, A.N. Akkara, C.G. Gonzales, M.C. Combe, P.M.W. Gill, B. Johnson, W. Chem, M.W. Wong, J.L. Andres, C. Gonzales, M. Head-Gordon, E.S. Replogle, J.A. Pople, GAUSSIAN 98, Revision A. 6, Gaussian Inc., Pittsburgh PA, 1998.

[24] H.B. Schlegel, M.J. Frisch, Int. J. Quantum Chem. 54 (1995) 83.

[25] V. Barone, M. Cossi, J. Phys. Chem. A 102 (1998) 1995.

[26] V. Sathyanarayanamoorthi, U. Ponnambalam, S. Gunasekaran, V. Kannappan, J. Mol. Liquids 112 (2004) 157.

[27] Y. Apeloig, R. Pauncz, M. Karni, R. West, W. Steiner, D. Chapman, Organometallics 22 (2003) 3250–3256.

[28] P.P. Gaspar, M. Xiao, D.H. Pae, D.J. Berger, T. Haile, T. Chen, D. Lei, W.R. Winchester, P. Jiang, J. Organomet. Chem. 646 (2002) 68.

[29] C. Gonzalez, A. Restrepo-Cossio, M. Márquez, K.B. Wiberg, M.D. Rosa, J. Phys. Chem. A 102 (1998) 2732–2738.

[30] K.J. Balasubramanian, Chem. Phys. 89 (1988) 5731.